Spectroscopic Characterization of Porphyrin Monolayer Assemblies

G. Alan Schick,*,† Irwin C. Schreiman, Richard W. Wagner, Jonathan S. Lindsey, and David F. Bocian*

Contribution from the Department of Chemistry, Carnegie Mellon University, 4400 Fifth Avenue, Pittsburgh, Pennsylvania 15213. *Received July 25, 1988*

Abstract: Supported monolayer assemblies containing free-base 5,10,15,20-tetrakis[4-(1-octyloxy)phenyl]porphyrin and the corresponding Cu(II), Zn(II), and Co(II) complexes have been investigated by using resonance Raman spectroscopy, polarized absorption and transmission spectroscopy, and fluorescence spectroscopy. For all of the complexes, the B-state absorptions are split in the monolayers with components red-shifted (~440 nm) and blue-shifted (~400 nm) relative to the solution values (~420 nm), whereas the Q-state absorptions are essentially unaltered. The spectral data are interpreted in terms of exciton interactions between the porphyrin B $\pi\pi^*$ excited states and are used to deduce a structural model for the arrangement of the porphyrin macrocycles in the monolayers. The porphyrins exist in domains comprised of at least seven molecules. The members of the domains are oriented approximately on-edge in a stack-of-cards configuration and are separated by ~4-5 Å, slipped by ~47° with respect to one another, and tilted (in a domain-fixed axis system) by ~40°. The domains are rotated ~13° about an axis which is parallel to the surface of the glass slide. This rotation effectively tips the macrocycles slightly off-edge.

Photosynthetic proteins contain ordered assemblies of porphyrinic molecules (chlorophylls) which serve as the active species in the initial steps of light-energy conversion.[1] The electronic structure of these assemblies facilitates extremely fast, vectorial electron transfer during the primary charge separation.[2] The unique properties of porphyrins suggest that synthetic assemblies of these and related compounds may be potentially useful as photoconductors, optical actuators, and chemical sensors.[3-8] Indeed, unusually large conductivities have been found in bridged and stacked phthalocyanine aggregates.[9-16] Consequently, the elucidation of the structural organization and photophysical properties of porphyrinic molecules in ordered molecular assemblies is a topic of current interest.[17]

Self-assembly processes such as micellization and insoluble-monolayer techniques provide a means for constructing organized molecular assemblies containing large numbers of noncovalently linked molecules. The photochemistry of porphyrins and metalloporphyrins in micelles and vesicles has been investigated by Whitten and co-workers.[18-22] More recently, the electrical and spectroscopic properties of porphyrins in solid, thin films have been examined by various investigators.[5-7,23-28] The spectroscopic features exhibited by porphyrins in solid films are different from those of porphyrins in solution. These differences are often ascribed to electronic (exciton) interactions between the chromophores in the film environment.[3,8,23,24,29] At present, however, a detailed characterization of the structural arrangement of the molecules which leads to these interactions is not available.

In this paper, we report a detailed spectroscopic investigation of supported monolayer assemblies which contain free-base 5,10,15,20-tetrakis[4-(1-octyloxy)phenyl]porphyrin (H_2TOOPP) and the corresponding Zn(II), Cu(II), and Co(II) complexes (Figure 1). The spectroscopic properties of these films are exemplary of those observed previously for monolayer and multilayer assemblies containing other meso-substituted tetraarylporphyrins such as *meso*-tetraphenylporphyrin,[29] *meso*-tetra-4-pyridylporphyrin,[29] *meso*-tetraphenylporphyrin cis substituted with fatty acids,[23] and 5-(4-carboxyphenyl)-10,15,20-tritolylporphyrin.[8] The absorption spectra of solution and monolayer samples of the TOOPP series appear in Figure 2. The spectra of the monolayer samples are characterized by a doubled B (Soret) band with one absorption component shifted toward the red region (ca. 440 nm) and the other toward the blue region (ca. 400 nm) compared to the solution's B-state absorption (ca. 420 nm). In contrast, the Q-band spectral features are quite similar for the film and solution samples. Herein, we elucidate the origin of the B-state splittings observed in the films by using polarized, angle-resolved absorption

† Present address: Department of Chemistry, Virginia Polytechnic Institute and State University, Blacksburg, VA 24061.

(1) (a) Okamura, M. Y.; Feher, G.; Nelson, N. In *Photosynthesis*; Govindjee, Ed.; Academic Press: New York, 1982; pp 195-272. (b) Feher, G.; Okamura, M. Y. In *The Photosynthetic Bacteria*; Clayton, R. K., Sistrom, W. R., Eds.; Plenum Press: New York, 1978; pp 349-386.
(2) Witt, H. T. In *Light-Induced Charge Separation in Biology and Chemistry*; Gerischer, H., Katz, J. J., Eds.; Verlag Chemie: Weinheim, 1979; pp 303-330.
(3) Yamashita, K.; Kihara, N.; Shimidzu, H.; Suzuki, H. *Photochem. Photobiol.* **1982**, *35*, 1-7.
(4) Kampas, F. J.; Yamashita, K.; Fajer, J. *Nature* **1980**, *284*, 40-42.
(5) (a) Jones, R.; Tredgold, R. H.; Hoorfar, A. *Thin Solid Films* **1985**, *123*, 307-314. (b) Jones, R.; Tredgold, R. H.; Hoorfar, A.; Hodge, P. *Ibid.* **1984**, *113*, 115-128. (c) Jones, R.; Tredgold, R. H.; Hodge, P. *Ibid.* **1983**, *99*, 25-32.
(6) Beswick, R. B.; Pitt, C. W. *Chem. Phys. Lett.* **1988**, *143*, 589-592.
(7) Tredgold, R. H.; Young, M. C. J.; Hodge, P.; Hoorfar, A. *IEEE Proc.-I* **1985**, *132*, 151-156.
(8) (a) Bardwell, J. A.; Bolton, J. R. *Photochem. Photobiol.* **1984**, *40*, 319-327. (b) *Ibid.* **1984**, *39*, 735-746.
(9) Hoffman, B. M.; Ibers, J. A. *Acc. Chem. Res.* **1983**, *16*, 15-21 and references therein.
(10) (a) Martinsen, J.; Stanton, J. L.; Greene, R. L.; Tanaka, J.; Hoffman, B. M.; Ibers, J. A. *J. Am. Chem. Soc.* **1985**, *107*, 6915-6920. (b) Ogawa, M. Y.; Martinsen, J.; Palmer, S. M.; Stanton, J. L.; Tanaka, J.; Greene, R. L.; Hoffman, B. M.; Ibers, J. A. *Ibid.* **1987**, *109*, 1115-1121.
(11) Turek, P.; Petit, P.; Andre, J.-J.; Simon, J.; Even, R.; Boudjema, B.; Guillaud, G.; Maitrot, M. *J. Am. Chem. Soc.* **1987**, *109*, 5119-5122.
(12) Nohr, R. S.; Kuznesof, P. M.; Wynne, K. J.; Kenney, M. E.; Siebenman, P. G. *J. Am. Chem. Soc.* **1981**, *103*, 4371-4377.
(13) Diel, B. N.; Inabe, T.; Lyding, J. W.; Schoch, K. F., Jr.; Kannewurf, C. R.; Marks, T. J. *J. Am. Chem. Soc.* **1983**, *105*, 1551-1567.
(14) Pietro, W. J.; Marks, T. J.; Ratner, M. A. *J. Am. Chem. Soc.* **1985**, *107*, 5387-5391.
(15) Diel, B. N.; Inabe, T.; Taggi, N. K.; Lyding, J. W.; Schneider, O.; Hanack, M.; Kannewurf, C. R.; Marks, T. J.; Schwartz, L. H. *J. Am. Chem. Soc.* **1984**, *106*, 3207-3214.
(16) Collman, J. P.; McDevitt, J. T.; Leidner, C. R.; Yee, G. T.; Torrance, J. B.; Little, W. A. *J. Am. Chem. Soc.* **1987**, *109*, 4606-4614.
(17) Honeybourne, C. L. *J. Phys. Chem. Solids* **1987**, *48*, 109-141.
(18) Barber, D. C.; Whitten, D. G. *J. Am. Chem. Soc.* **1987**, *109*, 6842-6844.
(19) Freitag, R. A.; Barber, D. C.; Inoue, H.; Whitten, D. G. *ACS Symp. Ser.* **1986**, *321*, 280-297.
(20) Krieg, M.; Whitten, D. G. *J. Am. Chem. Soc.* **1984**, *106*, 2477-2479.
(21) Cox, G. S.; Whitten, D. G. *Adv. Exp. Med. Biol.* **1983**, *160*, 279-292.
(22) Whitten, D. G.; Schmehl, R. H.; Foreman, T. K.; Bonilha, J.; Sobol, W. *ACS Symp. Ser.* **1981**, *177*, 38-51.
(23) (a) Möhwald, H.; Miller, A.; Stich, W.; Knoll, W.; Ruaudel-Teixier, A.; Lehmann, T.; Fuhrhop, J.-H. *Thin Solid Films* **1986**, *141*, 261-275. (b) Miller, A.; Knoll, W.; Möhwald, H.; Ruaudel-Teixier, A. *Ibid.* **1985**, *133*, 83-91.
(24) Ringuet, M.; Gagnon, J.; Leblanc, R. M. *Langmuir* **1986**, *2*, 700-704.
(25) Luk, S. Y.; Mayers, F. R.; Williams, J. O. *J. Chem. Soc., Chem. Commun.* **1987**, 215-216.

0002-7863/89/1511-1344$01.50/0

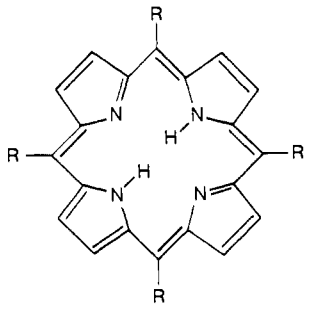

Figure 1. Structure of 5,10,15,20-tetrakis[4-(1-octyloxy)phenyl]-porphyrin (H_2TOOPP).

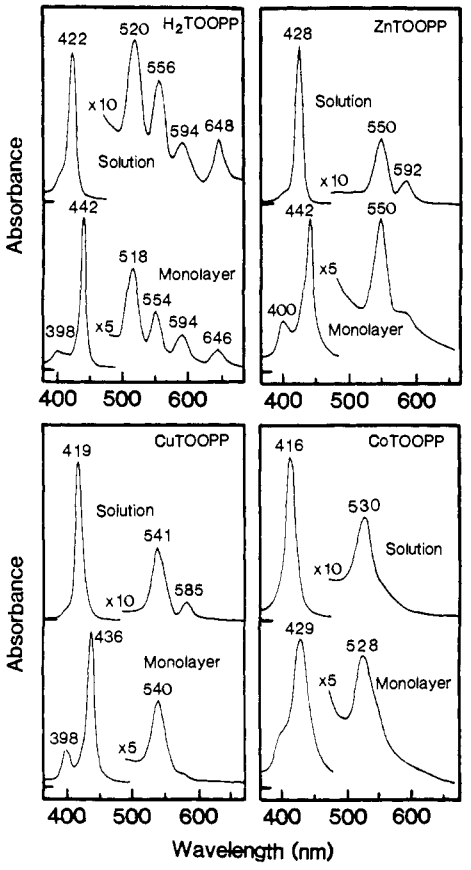

Figure 2. Absorption spectra of TOOPP complexes in $CHCl_3$ solutions and in 1:1 mixed monolayer assemblies with 1-(octyloxy)benzaldehyde (OOB). The spectra are normalized for the B-state maxima.

and transmission spectroscopy, fluorescence excitation and emission spectroscopy, and resonance Raman (RR) spectroscopy. On the basis of these spectral data, we propose a model for the organization of the porphyrin molecules in the monolayer assemblies.

Experimental Methods

Porphyrin Synthesis and Purification. Free-base 5,10,15,20-tetrakis-[4-(1-octyloxy)phenyl]porphyrin was synthesized as described elsewhere.[30] The Zn(II), Cu(II), and Co(II) complexes were prepared from the free-base compound and purified according to standard methods.[31]

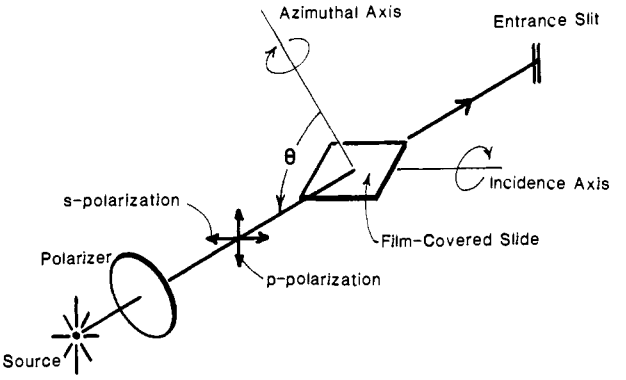

Figure 3. Experimental configuration for polarized angle-resolved absorption/transmission measurements.

The porphyrin compounds were estimated to be ≥99% pure by absorption and emission spectroscopy and by thin-layer chromatography. Solvents used for spectroscopic measurements and for monolayer deposition were HPLC grade (Fisher Scientific) and were used without further purification.

Monolayer Preparation. Insoluble monolayer assemblies were formed at an air/water interface by using standard methods.[32] Surface-area control (constant perimeter barrier type) and surface-pressure measurement (Wilhelmy-plate method), as well as the mechanism for transferring the films to solid substrates, were provided by a computer-controlled Joyce–Loebl Langmuir IV system. The trough is constructed of virgin Teflon with a stainless steel frame such that the subphase comes into contact only with materials of Teflon, the Wilhelmy plate (rigorously cleaned filter paper), and the solid substrate. Ultrapure water for the subphase was provided by a Zenopure filter system (Peck Water, Inc.) which produces water having a resistivity of >15 MΩ and levels of surfactants and dissolved organics which are undetectable by standard techniques.[33]

The monolayers were formed by spreading the porphyrins from chloroform solutions (~1 mg/mL) onto a pure water subphase (22 °C, pH 6.5). Accurate concentrations were determined from the optical absorptivities of the chloroform solutions. Monolayer films were transferred to glass substrates by standard dipping methods.[34] Hydrophilic glass cover slips (cleaned as described by Cross et al.[35]) were withdrawn from a subphase covered by a porphyrin film compressed to and maintained at the desired surface pressure. A transfer ratio of 1.0 (±0.05) was obtained for a dipping rate of 10 mm/min. For the angle-resolved optical transmission studies (see below) the monolayer-covered slides were cleaned on one side by carefully wiping with chloroform-dampened cotton swabs in order to allow measurements to be made on single monolayer assemblies.

Absorption and Transmission Spectroscopy. Polarized angle-resolved optical transmission studies were performed on monolayer films by attaching film-covered (one side only) slides to a rotation-stage assembly. The latter allows variation of both the incidence and azimuthal angles of the film plane relative to the electric vector of the source light beam. The experimental configuration is illustrated in Figure 3. A clean slide positioned at the equivalent angle values was used as the reference. Absorption and transmission spectra were obtained with the rotation-stage assembly in either a Hewlett-Packard Model 8541A diode-array spectrometer or in a Perkin-Elmer Model 330 grating spectrometer. Linear polarization of the source beam was achieved with a visible-wavelength sheet polarizer (Melles Griot), which maintains a polarizing extinction ratio of >500:1 throughout the range 350–650 nm.

Excitation and Emission Spectroscopy. Fluorescence excitation and emission spectra were recorded with a Gilford Fluoro IV spectrofluorimeter. The film-covered slide was positioned into a cuvette sample holder so that the exciting radiation impinged at an angle of ~30° from

(26) Bohorquez, M.; Patterson, L. K.; Brault, D. *Photochem. Photobiol.* **1987**, *46*, 953–957.
(27) Seta, P.; Bienvenue, E.; D'Epenoux, B.; Tenebre, L.; Momenteau, M. *Photochem. Photobiol.* **1987**, *45*, 137–143.
(28) Nagamura, T.; Matano, K.; Ogawa, T. *J. Phys. Chem.* **1987**, *91*, 2019–2021.
(29) (a) Bulkowski, J. E.; Bull, R. A.; Sauerbrunn, S. R. *ACS Symp. Ser.* **1981**, *146*, 279–293. (b) Bull, R. A.; Bulkowski, J. E. *J. Colloid Interface Sci.* **1983**, *92*, 1–12.
(30) Lindsey, J. S.; Schreiman, I. C.; Hsu, H. C.; Kearney, P. C.; Marguerattaz, A. M. *J. Org. Chem.* **1987**, *52*, 827–836.
(31) Fuhrhop, J.-H.; Smith, K. M. In *Porphyrins and Metalloporphyrins*; Smith, K. M., Ed.; Elsevier: Amsterdam, 1975; pp 757–869.
(32) Gaines, G. L., Jr. *Insoluble Monolayers at Liquid-Gas Interfaces*; Wiley-Interscience: New York, 1966.
(33) Mingins, J.; Owens, N. F. *Thin Solid Films* **1987**, *152*, 9–28.
(34) Kuhn, H.; Möbius, D.; Bücher, H. In *Techniques of Chemistry*; Weissberger, A., Rossiter, B. W., Eds.; Wiley-Interscience: New York, 1972; Vol. 1, Part IIIB, pp 577–702.
(35) Cross, G. H.; Peterson, I. R.; Girling, I. R.; Cade, N. A.; Goodwin, M. J.; Carr, N.; Sethi, R. S.; Marsden, R.; Gray, G. W.; Lacey, D.; McRoberts, A. M.; Scrowston, R. M.; Toyne, K. J. *Thin Solid Films* **1988**, *156*, 39–52.

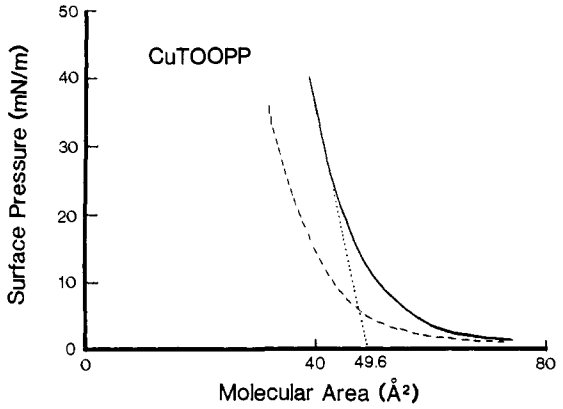

Figure 4. Pressure-area (π-A) curves obtained upon compression of CuTOOPP in pure (-) and mixed (--; 1:1 with OOB) monolayers at an air/water interface.

the film normal and so that the specular reflection was directed away from the detector slit. The emission was monitored at 90° to the incident beam. The monitored intensity was sensitive to the positioning of the slide in the sample compartment, but the slides could be repositioned consistently to give identical intensity readings to within 5%. Both emission and excitation spectra were recorded at rates of 100 nm/min with a spectral resolution of 5 nm and a detector responsivity of 1 s.

Resonance Raman (RR) Spectroscopy. RR spectra were acquired by using a computer-controlled Spex Industries Ramalog 9 macro Raman system equipped with a thermoelectrically cooled Hamamatsu R928 photomultiplier tube and photon-counting electronics. Excitation wavelengths were provided by the discrete lasing lines of krypton ion (Coherent Radiation Model K2000) and argon ion (Coherent Radiation Model Innova 15UV) lasers. A film-covered slide (1 monolayer on each side) was held so that the excitation beam was incident along the film normal. Scattered light trapped in the slide by total internal reflection emerged from the slide edge and was focused onto the entrance slit of the monochromator. RR spectra were recorded at 2-cm^{-1} intervals with an integration time of 5 s/point. Incident powers were typically 50 mW, and the spectral resolution was 6 cm^{-1}.

Results

Monolayer Films. It is now well-established that unsubstituted *meso*-tetraphenylporphyrin (TPP) complexes do not form stable monolayer films in pure form at gas/liquid interfaces.[29] However, long-chain amphiphilic substituents on the phenyl groups are often adequate to stabilize pure porphyrin films.[23,29,36] The TOOPP complexes represent an intermediate case. Pressure-area (π-A) isotherms measured for any of the pure TOOPP complexes at an air/water interface are indicative of a liquid-expanded phase with no obvious collapse for surface pressures to 40 mN/m (Figure 4). Extrapolated molecular areas for the complexes are 50 ± 1 Å^2. However, films maintained at surface pressures above 15 mN/m (25 °C, relative humidity 75%) develop visible folds and wrinkles over time (~1 h), indicating a slow collapse of the monolayer structure. The collapse can be completely inhibited by the addition of a surfactant species, 4-(1-octyloxy)benzaldehyde (OOB), in molar ratios near 1:1 with the respective TOOPP complex. Similar methods have been used to stabilize films of other meso-substituted tetraarylporphyrin complexes.[23,29] (It should be noted that the addition of OOB must be made to the spreading solution rather than to the expanded monolayer material at the air/water interface. Spreading the OOB and TOOPP materials separately causes the formation of macroscopic islands, as has been observed previously for other porphyrin monolayer systems.[29])

The incorporation of OOB into the TOOPP assemblies alters the physical characteristics of the monolayers. The *pure* (no OOB) films are "solid" to such an extent that removal of film material at the transfer site does not register at the pressure sensor (Wilhelmy plate) for periods documented up to 1 h. Such behavior is indicative of strongly aggregating species. Conversely, the mixed

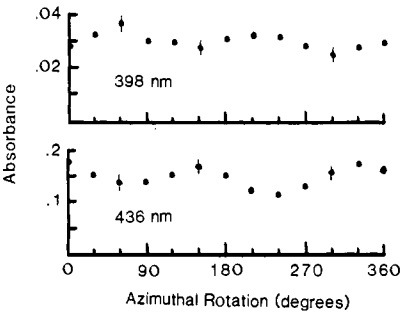

Figure 5. Azimuthal dependence of A_{max} for the 398- and 436-nm absorption bands of supported CuTOOPP:OOB (1:1) monolayer assemblies.

(including OOB) monolayers are more "fluid" than are those of pure TOOPP complexes, so reorganization in the films is much more rapid in response to surface pressure changes. As a result, the Wilhelmy-plate sensor responds to monolayer removal and the mixed monolayers transfer more uniformally.

Despite the dramatic effects the OOB has on the assembly properties of TOOPP monolayers, the spectroscopic properties of the films are unaffected. The absorption spectra of freshly prepared pure TOOPP monolayers exhibit the same features as those shown in Figure 2 for the mixed monolayer samples. These spectral features are different than those of collapsed monolayers. The spectra of collapsed films exhibit additional features which match those of the solution-phase spectra. The relative intensities of these additional features vary with experimental conditions and seem to parallel the extent of visible collapse of the films on the water surface. The similarities in the absorption spectra of the mixed and pure TOOPP monolayers imply that the structures of the organized species are unaltered by the inclusion of OOB surfactant molecules. Accordingly, the organized species appear to be stable porphyrin domains (aggregates) which behave as independent moieties. This characterization is supported by the observation that the features in the spectra of the mixed monolayers are invariant to deposition surface pressure (range 10-35 mN/m) and to the relative molar ratios of TOOPP:OOB (range 2:1-1:5). Thus, the species which are responsible for the observed absorption characteristics (Figure 2) are stable structures which form spontaneously on the water surface.

Absorption and Transmission Spectra. The B-state absorption of the porphyrin monolayers is split into two components whereas the Q-state absorption origin remains a single feature (Figure 2). This observation suggests that the B-state splitting is due to exciton interactions rather than to two different species in the film environment. Exciton splittings are proportional to the oscillator strength of the transition; consequently, B-state exciton interactions will be much larger than Q-state interactions.[37] In contrast, inhomogeneities in the film environment, which would give rise to multiple absorption maxima, would be expected to influence both the B and Q states.[38]

In order to investigate the characteristics of the two B-state absorption features observed for the TOOPP monolayers, we obtained polarized angle-resolved optical data from the supported assemblies (refer to Figure 3). Figure 5 shows a plot of the absorbance (A_{max}) of linearly polarized incident radiation as a function of the azimuthal angle, ϕ, for both the 436-nm and 398-nm absorption bands of the CuTOOPP assembly (normal incidence, $\theta = 0°$). Neither band exhibits a null absorbance for any value of ϕ, indicating that the transition dipoles for both contain components parallel to the plane of the film (in-plane). The intensity plots for both bands do exhibit definite oscillatory patterns with periods of approximately π and a phase shift of $\pi/2$ between the plots. The oscillations reveal that there exists an

(36) Ruaudel-Teixier, A.; Barraud, A.; Belbeoch, B.; Roulliay, M. *Thin Solid Films* **1983**, *99*, 33-40.

(37) Gouterman, M.; Holten, D.; Lieberman, E. *Chem. Phys.* **1977**, *25*, 139-153.

(38) (a) Gouterman, M. In *The Porphyrins*; Dolphin, D., Ed.; Academic Press: New York, 1978; Vol. III, pp 1-165. (b) Kim, D.; Holten, D.; Gouterman, M. *J. Am. Chem. Soc.* **1984**, *106*, 2793-2798.

anisotropic distribution of in-plane transition dipoles. The $\pi/2$ phase shift between the two plots indicates that the corresponding transition moments are correlated and further suggests that the two transitions are assignable to a single species. Results equivalent to these (not shown) were obtained for supported monolayers containing the free-base, Zn(II), and Co(II) derivatives of TOOPP.

The components of the transition dipoles which lie perpendicular to the film plane (out-of-plane) can be investigated via incidence angle dependence studies. However, measurements of the incidence-angle dependence of absorption intensities are complicated by interferences from wavelength and incidence angle dependent reflectivities of the monolayers. These complications arise from dispersion in the film refractive index. A procedure for quantitating the angular distribution of transition dipoles in monolayer and multilayer assemblies has been developed by Möbius and co-workers.[39,40] By this method, the optical properties of the assemblies are measured as

$$\Delta T_\sigma = 1 - T_m/T_g \quad (1)$$

where T_m and T_g are the optical transmission of the monolayer-covered and clean glass slides, respectively. The σ subscript on ΔT denotes the polarization of the incident light (s- or p-polarized, see Figure 3). In using this procedure, the quantity $\Delta T_s/\Delta T_p$ is an incidence angle dependent, absorptivity-dependent quantity which is related to the angular distribution of the out-of-plane transition dipoles in the film. For molecular aggregates which are much smaller than visible wavelengths and for which the out-of-plane transition dipoles are distributed randomly about the surface normal, the average tilt angle, θ, of the transition moments may be obtained by determining the order parameter, $P(\theta) = \langle \cos^2 \theta \rangle$. By use of this definition of the order parameter, $P(\theta) = 0$ or 1 for purely in-plane or out-of-plane transition dipoles, respectively, and $P(\theta) = 0.33$ for an isotropic distribution. The relationship between $P(\theta)$ and the experimental quantity $\Delta T_s/\Delta T_p$ has been evaluated by Orrit et al. for various incidence angles and absorptivity conditions.[39]

The plots shown in Figure 5 indicate a nonrandom distribution of in-plane transition-dipole components. Accordingly, the out-of-plane components are not distributed randomly about the surface normal. This greatly complicates the determination of $P(\theta)$. However, we have found that monolayer assemblies containing CuTOOPP can be made which exhibit no azimuthal angle absorption variance (random distribution). These monolayers are formed by starting the deposition process at the prescribed surface pressure before the film at the air/water interface is allowed to relax completely to a stable area reading. Films deposited in this manner exhibit spectral features identical with those representing the stabilized assemblies, thereby suggesting that pretransfer equilibration of the monolayer-film area corresponds mechanistically to an organization of the in-plane orientation of the preformed aggregates.

Measurements of ΔT_σ for the azimuthally absorption-invariant assembly containing CuTOOPP are shown in Figure 6. The intensities of the bands at 436 and 398 nm exhibit quite different angular dependences. The intensity of the 436-nm band, which is largest at normal incidence ($\theta = 0°$), diminishes as θ is varied whereas that of the 398-nm band increases. For $\theta > 70°$ (not shown) the intensity of the 398-nm band exceeds that of the 436-nm band. The values of $\Delta T_s/\Delta T_p$ are 1.28 and 0.64 for the 436- and 398-nm transitions, respectively. These values correspond to $P(\theta) \approx 0.030$ and 0.40.[39] Identical results (to within 7%) are obtained for all the assemblies containing the TOOPP derivatives, including the azimuthally absorption variant monolayers (after averaging the azimuthal variance). The value of $P(\theta)$ for the 436-nm absorption band is close to that expected for purely in-plane transition dipoles [$P(\theta) = 0$]. On the other hand, the value of $P(\theta)$ for the 398-nm band is only slightly larger than that expected for an isotropic distribution of out-of-plane transition dipoles [$P(\theta) = 0.33$].

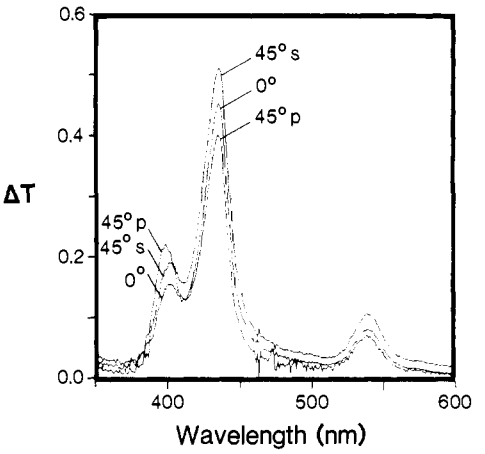

Figure 6. Incidence-angle (θ) dependence of ΔT (see the text) for supported CuTOOPP:OOB (1:1) monolayer assemblies. The corresponding polarizations (s or p) and values of θ are indicated for each curve.

The occurrence of a nearly isotropic distribution of out-of-plane transitions would imply that some domains exist in which the porphyrins stand on-edge whereas other domains exist in which the macrocycles lie flat on the surface of the glass slide. This latter case is highly implausible and inconsistent with the measured molecular areas. An isotropic distribution of out-of-plane dipoles would also imply that the 398-nm absorption feature contains contributions from domains in which the molecules are tilted over a wide range of angles. This is implausible in the context of the exciton model because the absorption energy varies substantially with tilt angle (vide infra). Yet, the 398-nm band is comparable in width to the 436-nm band, and both are essentially identical in width with the B-state absorption band of dilute solution samples (Figure 2). An alternative and more reasonable interpretation is that the value $P(\theta) = 0.40$ reflects a narrow distribution of out-of-plane angles for which the average tilt angle is commensurate with the measured $P(\theta)$. This angle is $\sim 50°$. Similarly, the value of $P(\theta) = 0.030$ measured for the 436-nm band would correspond to an average tilt angle of $\sim 80°$. The estimated errors for the measured values of $P(\theta)$ result in errors of approximately $\pm 1°$ in the predicted average tilt angles.

Emission and Excitation Spectra. Quenching of the Q-state emission from mixed-monolayer films containing both fluorescent and nonfluorescent species can be used to deduce the extent of aggregation in the monolayers. Such procedures have been used to determine the extent of aggregation in monolayer assemblies containing organic dyes.[41] If the exciton interactions between the molecules are strong, a domain containing at least one nonfluorescent species will not fluoresce. Because Q-state emission of Cu(II) porphyrins is quenched via intersystem crossing into a tripdoublet state,[38] mixed monolayers containing both ZnTOOPP and CuTOOPP should exhibit fluorescence from only aggregates of pure ZnTOOPP. Accordingly, the observed fluorescence intensity will be proportional to the fraction of pure ZnTOOPP domains present in the films. The optical absorption results have revealed that aggregation in the TOOPP films is governed by porphyrin–porphyrin interactions and is metal independent. Therefore, supported mixed monolayers containing TOOPP complexes of Zn(II) and Cu(II) should contain a purely statistical distribution of aggregates described by $(\text{ZnTOOPP})_x(\text{CuTOOPP})_{N-x}$, where $0 \le x \le N$ (N is the aggregation number) and the relative abundance of each aggregate species is given by a concentration-weighted binomial distribution of order N. In general, for a monolayer assembly containing ZnTOOPP:CuT-

(39) Orrit, M.; Möbius, D.; Lehmann, U.; Meyer, H. *J. Chem. Phys.* **1986**, *85*, 4966–4979.
(40) Grüniger, H.; Möbius, D.; Meyer, H. *J. Chem. Phys.* **1983**, *79*, 3701–3710.
(41) (a) Kuhn, H. In *Light-Induced Charge Separation in Biology and Chemistry*; Gerischer, H., Katz, J. J., Eds.; Verlag Chemie: Weinheim, 1979; pp 151–169. (b) Kuhn, H. *J. Photochem.* **1979**, *10*, 111–132.

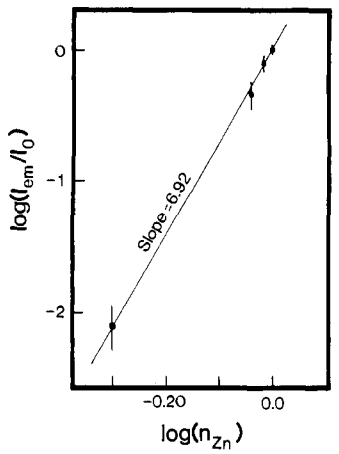

Figure 7. Mole-fraction dependence of the Q-state fluorescence intensity of ZnTOOPP in mixed monolayer assemblies containing CuTOOPP.

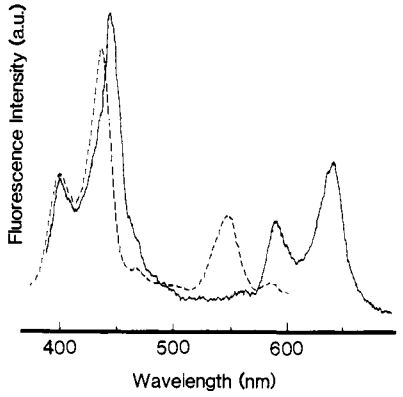

Figure 8. Emission (–; λ_{em} = 360 nm) and excitation (- -; λ_{ex} = 640 nm) spectra obtained from supported ZnTOOPP:OOB (1:1) monolayer assemblies.

OOPP with a ZnTOOPP mole fraction n_{Zn}, the relative fluorescence intensity is given by

$$(I_{em}/I_0) = (n_{Zn})^N \quad (2)$$

where I_0 is the emission intensity observed for a monolayer assembly containing $n_{Zn} = 1$. The aggregation number, N, is then determined as the slope of a line extracted from a plot of log (I_{em}/I_0) vs log (n_{Zn}). Figure 7 shows a log–log plot of the Q-state fluorescence intensity vs n_{Zn} for ZnTOOPP:CuTOOPP monolayers. The data correlate well with a slope corresponding to an aggregation number of seven. This represents a lower bound on the aggregation number. Interpretations of the data based on the relative rate constants of radiative and nonradiative relaxation mechanisms predict slightly larger values ($N \approx 12$).[41] Regardless, it is evident that the TOOPP domains in the monolayer assemblies are substantially larger than dimeric species.

In the course of the studies to determine the aggregation number, we observed some unusual features in the excitation and emission spectra of all the films. These unusual features are illustrated in the fluorescence excitation and emission spectra of ZnTOOPP monolayers which appear in Figure 8. Strong fluorescence is observed from both the B and Q states of the monolayer assemblies. This is in dramatic contrast to normal solution-phase fluorescence from porphyrins, which originates primarily from the Q state.[38] B-state fluorescence is not well characterized, although triplet–triplet annihilation has been proposed as a possible mechanism.[42,43] Such a mechanism should be enhanced in highly aggregated assemblies.[43] The fluorescence spectra of monolayer assemblies containing H_2TOOPP (not shown) also exhibit enhanced B-state fluorescence. More interestingly, the monolayers of CuTOOPP also exhibit B-state fluorescence. As yet, we have not quantitated the monolayer B-state fluorescence intensities nor have we examined the polarization characteristics. These data are clearly needed in order to elucidate the nature of the unusual B-state emission.

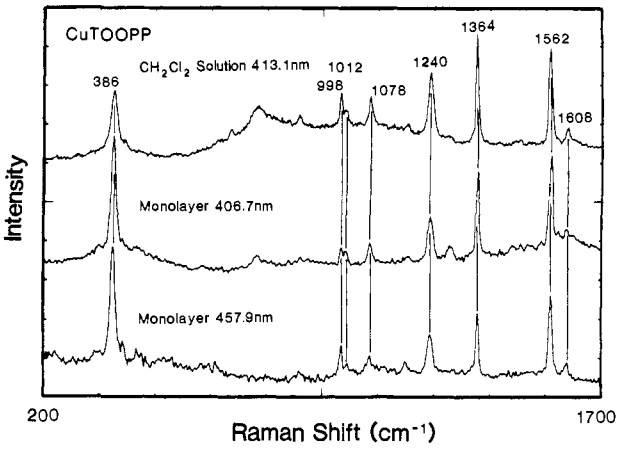

Figure 9. B-state excitation RR spectra of CuTOOPP in CH_2Cl_2 solution and mixed-monolayer assemblies (1:1 with OOB). Excitation wavelengths are indicated.

RR spectra. As an independent probe of the film species which give rise to the two B-state absorption bands, we obtained RR spectra of the films with excitation into the two different bands. The RR spectra obtained for a CuTOOPP monolayer assembly are shown in Figure 9. Also shown is the RR spectrum of CuTOOPP in CH_2Cl_2 solution obtained with excitation in resonance with the 420-nm B-state absorption band (see Figure 2). The spectra observed with excitation into the two different B-state absorptions of the film are essentially identical. In addition, the vibrational frequencies of the molecules in the monolayer are nearly identical with those of free CuTOOPP in dilute solution. These data further confirm that the two B-state absorptions arise from the same species and show that the structures of the porphyrins are essentially unperturbed in the monolayer environment.[44] Collectively, these observations indicate that the spectral properties of the aggregate species in the monolayers are dominated by electronic, rather than by structural, perturbations. Analogous results are obtained for monolayer assemblies containing ZnTOOPP (not shown).

Discussion

The spectral data reported here lend insight into the general structural features of the porphyrin monolayers. The general properties of the films are as follows: (i) the structures of the individual molecules differ negligibly from those of the free complexes in dilute solution, (ii) the porphyrins exist in domains comprised of at least seven strongly interacting (electronically) molecules, and (iii) the orientational distribution of the domains is determined by the conditions under which the monolayer is formed. The observation that the preferred distribution of domains is anisotropic suggests that preparative conditions may be found for achieving even more uniform macroscopic order.

The spectral data can be used to quantitate the geometrical arrangement of the molecules in the domains. In an exciton model, the B-state splittings in the absorption spectra are determined by the center–center distances between the interacting dipoles, their relative orientations, the oscillator strengths of the monomer transitions, and the number of monomers in the domains.[45,46] The simplest possible domain is a dimer for which the transition energies to the exciton-split states are given by

$$E_{dimer} = E_{monomer} + D \pm \epsilon \quad (3)$$

(42) Frink, M. E.; Ferraudi, G. *Chem. Phys. Lett.* **1986**, *124*, 576–578.
(43) Stelmakh, G. F.; Tsvirko, M. P. *ACS Symp. Ser.* **1986**, *321*, 119–127.
(44) Spiro, T. G. In *Iron Porphyrins*; Lever, A. P. B., Gray, H. B., Eds.; Addison-Wesley: Reading, MA, 1982; Part II, pp 89–159.
(45) Kasha, M.; Rawls, H. R.; El-Bayoumi, M. A. *Pure Appl. Chem.* **1965**, *11*, 371–392.
(46) Kasha, M. *Radiat. Res.* **1963**, *20*, 55–71.

where $E_{monomer}$ is the transition energy of the monomer species, D is dispersion energy term, and ϵ is the exciton interaction energy, which corresponds to the off-diagonal elements of the 2 × 2 coupling matrix

$$\epsilon = |M|^2/(r_{cc})^3\, g(\alpha,\beta,\gamma) \quad (4)$$

Here, M is the monomer transition dipole moment, r_{cc} is the distance between the centers of the interacting transition dipoles, and $g(\alpha,\beta,\gamma)$ is an orientation function. In the case of parallel transition dipoles, the orientation function is given by

$$g(\eta) = 1 - 3\cos^2\eta \quad (5)$$

where η is the angle between the transition dipoles and a line connecting the dipole centers. For extended aggregates ($N > 2$) in which nearest-neighbor interactions dominate, the coupling matrix elements are also described by eq 4 and 5; however, the observed exciton splitting increases from 2ϵ ($N = 2$) to a limiting value of 4ϵ ($N = \infty$).

For the series of TOOPP monolayers, two B-state absorptions are observed—one shifted toward the red region and the other toward the blue region relative to the absorption maximum in solution. The red-shifted absorption is polarized nearly in-plane, whereas the blue-shifted absorption contains a substantial out-of-plane component (for convenience, we refer to these as in-plane and out-of-plane, respectively). The most plausible model for the individual domains which is consistent with both these data and the molecular area measurements is one in which the macrocycles sit on edge on the glass surface in a stack-of-cards arrangement (Figure 10). In such a model, the individual molecules can be tilted with respect to the monolayer normal and slipped with respect to one another. Similar models have been proposed previously for monolayer assemblies of porphyrins and phthalocyanines, although no detailed structural characterizations have been advanced.[23,47,48] In the stack-of-cards model, the two B-state absorption bands cannot arise from transitions to members of the same exciton manifold because the transition dipoles are parallel and only one transition is strongly allowed.[45] The incidence angle dependence studies reported above indicate that both observed B-state transitions are strongly allowed; therefore, the 398- and 436-nm bands must correspond to the strongly allowed transitions of two different exciton manifolds. The two manifolds arise because the monomer B states are doubly degenerate. It should be noted that an oblique (nonparallel) orientation of the transition dipoles would give rise to two allowed transitions from a single manifold.[45,46] However, for metalloporphyrins, oblique orientations would be expected to give rise to more than two observed transitions, owing to the degeneracy of the B state. Inasmuch as only two bands are observed, the oblique orientations would require that several bands are overlapping and cannot be resolved by the angular dependence studies. This seems highly unlikely. A more reasonable explanation, which is readily accommodated by a stack-of-cards model, is that the degeneracy in the B state is lifted by exciton interactons for which the angle between the line-of-centers and the in-plane dipoles, η_1, is different from that between the line-of-centers and the out-of-plane dipoles, η_2. For the monolayers studied here, the observation of the red- and blue-shifted absorption bands implies that η_1 and η_2 are less than and greater than the magic angle (54.7°), respectively.

A schematic representation of the stack-of-cards model is shown in Figure 10. The glass surface defines the XY plane in the laboratory frame. In this frame, the macrocycles can be slipped with respect to one another along the glass surface and/or tilted with respect to the monolayer normal (Figure 10, parts b and c). The angle η_1 corresponds to the slip angle whereas the angle η_2 is related to the tilt angle, Θ, by

$$\cos\eta_2 = \sin\eta_1 \sin\Theta \quad (6)$$

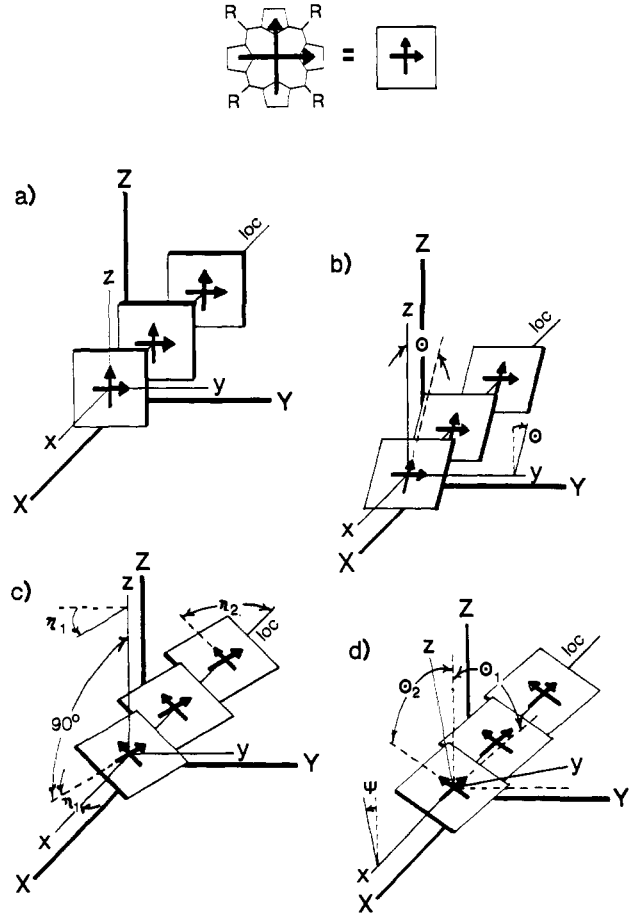

Figure 10. Structural model for the TOOPP monolayer domains. Both the laboratory frame (XYZ; the XY plane corresponds to the glass surface) and the domain-fixed reference frame (xyz) are shown. Only three molecules are depicted for clarity. The macrocycle arrangement is shown for (a) a face-to-face domain, (b) a domain tilted at the angle Θ about the y axis, (c) a tilted domain slipped through the angle η_1 about the z axis and (d) a tilted, slipped domain which is rotated by the angle ψ about the line of centers (loc; x axis). The angle η_2 and the experimentally measured angles Θ_1 and Θ_2 are also labeled.

In this description, one set of dipoles is rigorously in-plane whereas the orientation of the other is determined by Θ. However, the polarized transmission measurements indicate that the in-plane transition moment exhibits a small amount of out-of-plane character (~10°). Accordingly, eq 6 is not rigorously correct. A more appropriate coordinate system is one defined with respect to the domain where η_1 is constrained to the xy plane (in this coordinate system the "in-plane" transition dipoles are rigorously in-plane). This coordinate system is effectively rotated with respect to the laboratory frame. The only rotation which can account for the small tilt of the in-plane transition moment while preserving contact between the glass surface and all members of the domain (i.e., conserving the monolayer nature) is one about the line-of-centers. In the stack of cards model, this rotation lifts the molecules slightly off their edges (Figure 10d). The measured tilt angles of the in-plane and out-of-plane transition moments, Θ_1 and Θ_2, are related to the rotation angle, ψ, by

$$\cos\Theta_1 = -\sin\eta_1 \sin\psi \quad (7)$$

$$\cos\Theta_2 = \sin\psi \cos\eta_1 \sin\Theta' + \cos\psi\cos\Theta' \quad (8)$$

where Θ′ is defined as the tilt angle with respect to the z axis of the domain-fixed frame. Elimination of ψ between eq 7 and 8 yields

$$\cos\Theta_2 = -\cos\Theta_1 \cot\eta_1 \sin\Theta' + \left[1 - \frac{\cos^2\Theta_1}{\sin^2\eta_1}\right]^{1/2}\cos\Theta' \quad (9)$$

which relates the angles in the laboratory frame, Θ_1 and Θ_2, to

(47) Kovacs, G. J.; Vincett, P. S.; Sharp, J. H. *Can. J. Phys.* **1985**, *63*, 346–349.

(48) (a) Barger, W. R.; Snow, A. W.; Wohltjen, H.; Jarvis, N. L. *Thin Solid Films* **1985**, *133*, 197–206. (b) Hann, R. A.; Gupta, S. K.; Fryer, J. R.; Eyres, B. L. *Ibid.* **1985**, *134*, 35–42.

Table I. Structures of CuTOOPP Aggregates in Monolayer Assemblies

					dimer		heptamer		polymer	
E, cm^{-1} [a]	η_1, deg	η_2, deg	Θ', deg	ψ, deg	r_{cc} [b]	r_{ip} [c]	r_{cc} [b]	r_{ip} [c]	r_{cc} [b]	r_{ip} [c]
23 700	53.6	57.5	41.9	12.5	4.22	2.53	5.18	3.10	5.31	3.18
23 800	53.1	57.9	41.7	12.5	4.49	2.68	5.51	3.29	5.65	3.38
23 900	52.3	58.5	41.4	12.7	4.87	2.89	5.98	3.55	6.13	3.64
24 000	51.1	59.2	41.1	12.9	5.33	3.13	6.54	3.84	6.72	3.94
24 050	50.1	59.9	40.8	13.1	5.67	3.29	6.95	4.04	7.14	4.15
24 100 [d]	48.8	60.8	40.4	13.3	6.04	3.46	7.42	4.25	7.61	4.36
24 150	46.6	62.4	39.7	13.8	6.60	3.69	8.10	4.53	8.31	4.65
24 200	43.0	65.0	38.3	14.8	7.34	3.93	9.01	4.82	9.24	4.95
24 300	27.5	76.9	29.5	22.1	9.31	3.74	11.73	4.72	11.43	4.60
24 350	16.3	86.7	12.0	38.2	10.02	2.75	12.30	3.38	12.62	3.47

[a] $E = (E_{monomer} + D)$. [b] Calculated for the measured transition moment of CuTOOPP, M = 12.3 D. In Å. [c] $r_{ip} = r_{cc} \sin \eta_1 \sin \eta_2$. In Å. [d] E(3-methylpentane).

the angles in the domain frame, η_1 and Θ'. The remaining angle in the domain frame, η_2, is related to η_1 and Θ' by replacing Θ with Θ' in eq 6. The angles η_1 and η_2 are related to the exciton energies, ϵ_1 and ϵ_2, by eq 4 and 5:

$$\frac{\epsilon_1}{\epsilon_2} = \frac{(1 - 3\cos^2 \eta_1)}{(1 - 3\cos^2 \eta_2)} \tag{10}$$

Solving eq 10 for η_2 and substituting the expression into eq 6 yields a second equation relating η_1 and Θ':

$$\sin \Theta' = \left[\frac{3\cos^2 \eta_1 + (\epsilon_1/\epsilon_2) - 1}{3(\epsilon_1/\epsilon_2) \sin \eta_1} \right]^{1/2} \tag{11}$$

Elimination of Θ' between eq 9 and 11 yields the relationship between the unknown angle, η_1, and the measured parameters, Θ_1, Θ_2, ϵ_1, and ϵ_2:

$$\cos \Theta_2 = -\cos \Theta_1 \cot \eta_1 \left[\frac{3\cos^2 \eta_1 + (\epsilon_1/\epsilon_2) - 1}{3(\epsilon_1/\epsilon_2) \sin \eta_1} \right]^{1/2} + \left[1 - \frac{\cos^2 \Theta_1}{\sin^2 \eta_1} \right]^{1/2} \left[1 - \frac{3\cos^2 \eta_1 + (\epsilon_1/\epsilon_2) - 1}{3(\epsilon_1/\epsilon_2) \sin \eta_1} \right]^{1/2} \tag{12}$$

The angle η_2 can then be found from eq 10. The distance r_{cc} is related to the transition moment of the monomer through eq 4.

In order to solve eq 12, values must be obtained for ϵ_1 and ϵ_2. Because only one transition is observed for each exciton manifold, these energies must be estimated by an independent means. The exciton energies are related to the monomer transition energy and the dispersion energy by eq 3, but neither of these latter energies is explicitly known. An estimate of the monomer transition energy can be obtained by measuring the absorption maximum in a variety of solvents (these energies actually correspond to the gas-phase monomer energy as modified by the dispersion energy of the given solvent). The absorption maximum of CuTOOPP appears at 415 nm (~24 100 cm^{-1}) in hydrocarbon solvents such as 3-methylpentane, at 421 nm (~23 700 cm^{-1}) in aromatic solvents such as benzene, and near 419 nm (~23 900 cm^{-1}) in chlorinated solvents such as chloroform or methylene chloride. The solutions for eq 12 for several values of E ($= E_{monomer} + D$), which span the range of observed solution-phase transition energies, are given in Table I.

Inspection of Table I reveals that a lower bound on E is determined by the requirement that η_1 and η_2 must be less than and greater than 54.7°, respectively. The values of E are further constrained by the requirement that the interplanar separation, r_{ip}, is not unreasonably small (<4Å for *meso*-tetraarylporphyrins).[49] The E values in the range of those observed for aromatic and chlorinated solvents fall into this latter category. On the other hand, E values close to those observed for hydrocarbon solutions (24 100 ± 100 cm^{-1}) produce reasonable r_{ip} values (4–5 Å). These E values result in η_1 and η_2 values of 43°–50° and 60°–65°, respectively, and Θ' values near 40°. These values are also reasonable within the context of the molecular-area measurements. The small measured areas (~50 Å^2) require that the macrocycles are close enough together that tilting results in substantial overlap of adjacent rings. If $E >$ 24 300 cm^{-1} (>200 cm^{-1} higher than observed for a 3-methylpentane solution), the values of r_{ip} again become unreasonably small. For E ~24 300 cm^{-1}, the values of r_{ip} are reasonable (~4.6 Å); however, the values of η_1, η_2, and Θ' result in molecular areas which are inconsistent with the measured values. [These values might be possible in a monolayer which exhibits a high degree of two-dimensional order (an array-of-cards model); however, the spectral data indicate that this is not the case.] Similar geometrical parameters are obtained from analyses of the spectral data obtained for the Zn(II), Co(II), and free-base complexes of TOOPP.

Summary and Conclusions

The spectroscopic properties of monolayer assemblies containing H_2TOOPP and the corresponding Zn(II), Cu(II), and Co(II) complexes can be successfully interpreted in terms of exciton interactions between the B $\pi\pi^*$ states of neighboring chromophores. These chromophores exist in domains of at least seven molecules. The structures of the molecules in the monolayers are essentially unperturbed from those in dilute solution. A model which is consistent with the spectroscopic data is one in which the molecules in the domains are arranged in a stack-of-cards configuration. The members of the domain are separated by ~4–5 Å, slipped by ~47° with respect to one another, and tilted (in a domain-fixed axis system) by ~40°. The domains are rotated slightly (~13°) with respect to the surface of the glass slide. This rotation effectively tips the macrocycles off-edge.

The spectroscopic evidence presented here holds certain implications to previous studies of porphyrin assemblies. Similar observations have been made for monolayer and multilayer assemblies containing various meso-substituted tetraarylporphyrin complexes. The similarities in the spectral data suggest that *meso*-tetraarylporphyrin complexes tend to assemble into similar aggregate structures regardless of the exact nature of the aryl substituents. In addition, the aggregate structure is apparently independent of the metal ion, although only 4-coordinate metal complexes have been investigated. In this respect, it would be interesting to examine the effects of axial ligands on the formation and structures of porphyrins in solid assemblies. Certain types of axial ligands may promote the formation of large domains and hence macromolecular order. The ability to construct highly ordered macromolecular assemblies is a prerequisite for utilizing these assemblies for practical applications.

Acknowledgment. This work was supported by Grants GM-36243 (D.F.B.) and GM-36238 (J.S.L.) from the National Institute of General Medical Sciences and Grant No. 349 from the Western Pennsylvania Advanced Technology Center (D.F.B.).

(49) Boyd, P. D. W.; Smith, T. D.; Price, J. H.; Pilbrow, J. R. *J. Chem. Phys.* **1972**, *56*, 1253–1263.